

Identification of the $V_{\text{Al}}\text{-O}_{\text{N}}$ defect complex in AlN single crystals

J.-M. Mäki,^{1,*} I. Makkonen,¹ F. Tuomisto,² A. Karjalainen,³ S. Suihkonen,³ J. Räisänen,⁴
T. Yu. Chemekova,⁵ and Yu. N. Makarov⁶

¹*Helsinki Institute of Physics and Department of Applied Physics, Aalto University, P.O. Box 14100, FI-00076 Aalto, Espoo, Finland*

²*Department of Applied Physics, Aalto University, P.O. Box 11100, FI-00076 Aalto, Finland*

³*Department of Micro- and Nanosciences, Aalto University, P.O. Box 13000, FI-00076 Aalto, Espoo*

⁴*Accelerator Laboratory, University of Helsinki, P.O. Box 43, FI-00014, Helsinki, Finland*

⁵*GaN-Crystals, Ltd, St. Petersburg, Engels Avenue 27, 194156, Russia*

⁶*N-Crystals Group, St. Petersburg, Engels Avenue 27, 194156, Russia*

(Received 27 June 2011; published 29 August 2011)

In this Rapid Communication, we report positron annihilation results on in-grown and proton irradiation-induced vacancies and their decoration in aluminium nitride (AlN) single crystals. By combining positron lifetime and coincidence Doppler measurements with *ab initio* calculations, we identify in-grown $V_{\text{Al}}\text{-O}_{\text{N}}$ complexes in the concentration range 10^{18} cm^{-3} as the dominant form of V_{Al} in the AlN single crystals, while isolated V_{Al} were introduced by irradiation. Further, we identify the UV absorption feature at around 360 nm that involves V_{Al} .

DOI: [10.1103/PhysRevB.84.081204](https://doi.org/10.1103/PhysRevB.84.081204)

PACS number(s): 61.72.-y, 78.66.Fd, 78.70.Bj, 81.05.Ea

Aluminium nitride (AlN) is a promising extremely wide band-gap ($E_g = 6.2 \text{ eV}$) semiconductor for use in deep ultraviolet optoelectronics.¹ AlN can also be alloyed with other III nitrides in order to tailor the active wavelength from infrared to deep ultraviolet. To exploit the full potential of devices based on III nitrides, lattice-matched bulk substrates are needed in order to minimize the defects caused by lattice mismatch. This is driving the need to develop nitride growth methods capable of creating either true bulk crystals or several millimeter thick heteroepitaxial layers that can be separated from the substrate.^{2,3} Synthesis of large enough AlN single crystals has been difficult with problems ranging from threading dislocations to vacancy type point defects. Physical vapor deposition (PVT) has emerged as a method of choice for producing AlN single-crystal substrates.⁴⁻⁷ However, vacancy defects produced during the synthesis still play a major role in the general crystal quality. Vacancies in the AlN substrate can have a major impact on the device operation. For example, vacancy-impurity complexes have been reported to affect the thermal conductivity of the material,^{8,9} affecting the device operation. Also, it has been reported that point defects can cause UV absorption,¹⁰ which should be minimized in order to achieve effective light extraction through the substrate.

Positron annihilation spectroscopy is a powerful tool in studying cation vacancies in nitride semiconductors.^{11,12} A few reports on positron annihilation results in both bulk¹³ and thin film¹⁴⁻¹⁶ AlN exist, but conclusive evidence on the identity and decoration of the observed vacancies is missing. In this Rapid Communication, we report positron annihilation spectroscopy results on the identification of in-grown and irradiation-induced defects in PVT-grown bulk AlN crystals. We show that in as-grown AlN crystals, Al vacancies are present at a concentration in the range of 10^{18} cm^{-3} . The in-grown Al vacancies are complexed with oxygen ($V_{\text{Al}}\text{-O}_{\text{N}}$), while isolated V_{Al} can be produced by irradiation.

The measured bulk AlN crystals were grown by PVT at 2600 K in tungsten crucibles (for details, see Ref. 17).

300- μm -thick wafers were cut from the ingot for the measurement. Energy-dispersive x-ray spectroscopy (EDS) measurements show that the wafers contain less than 100 ppm impurities (10^{19} cm^{-3}) with gas discharge mass spectrometry (GDMS) showing at most 10 ppm of oxygen impurities (10^{18} cm^{-3}). Positron lifetime measurements were performed at temperatures between 20 and 750 K with conventional lifetime instrumentation.¹⁸ The increase of average positron lifetime τ_{ave} (the center of the mass of the spectrum) above the lifetime in the lattice of the material is an indication of vacancy defects being detected. The positron Doppler broadening experiments were performed using high-purity Ge detectors with energy resolution of 1.3 keV. When the positrons are trapped at vacancies, the probability of annihilation with high-momentum core electrons is reduced, narrowing the Doppler broadening spectrum. In order to identify the chemical surrounding of the vacancy, coincidence Doppler measurements were performed.¹⁸ The optical absorption and transmission spectra of the AlN films were measured with a xenon lamp, monochromator, and photomultiplier tube at room temperature.

We also calculated the positron-electron momentum density from first principles for vacancy defects and the AlN lattice. The valence electron densities were calculated self-consistently using the local-density approximation (LDA) employing the projector augmented wave (PAW) method¹⁹ and a plane-wave code VASP.²⁰ The Doppler spectra were calculated in the direction of the c axis of the wurtzite AlN with the relaxation caused by a positron to the vacancy taken into account. For details on the computational methods, see Ref. 21. Two of the AlN wafers were irradiated with 9.5 MeV protons to a fluence of 10^{16} cm^{-2} with a tandem accelerator.²² The energy of the protons is high enough to penetrate the 300- μm -thick wafer and generate a homogeneous defect profile, but low enough to create only monovacancies. From SRIM²³ calculations, we estimate that $4 \times 10^{18} \text{ cm}^{-3}$ Al vacancies and $3 \times 10^{18} \text{ cm}^{-3}$ N vacancies are generated for the irradiation fluence of 10^{16} cm^{-2} .

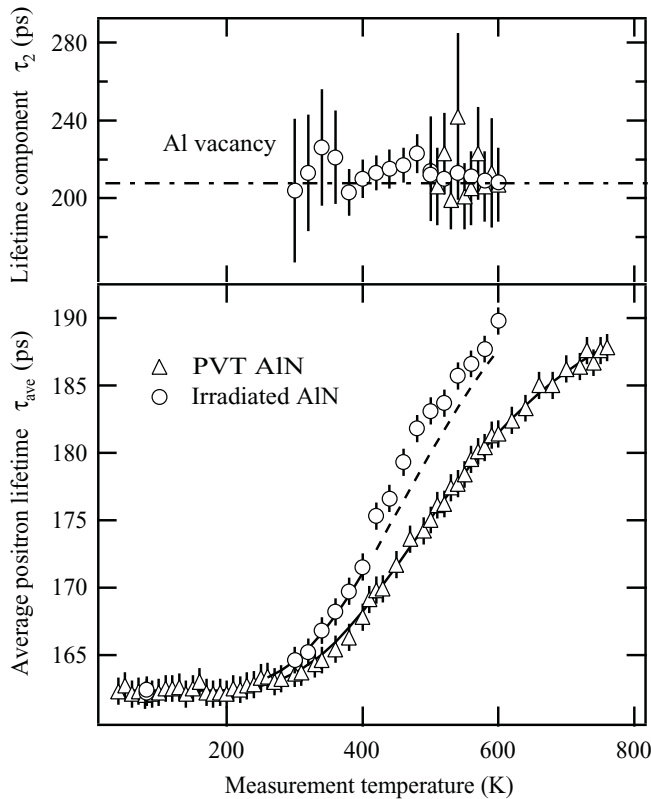


FIG. 1. Average positron lifetime as a function of measurement temperature and the second lifetime component, corresponding to the Al vacancy. Parameters used in the fit (the solid line) are $\tau_B = 157$ ps, $\tau_V = 210$ ps and $E_b = 140$ meV.

The average positron lifetime measured in an epi-ready polished wafer was 158 ps at room temperature (RT). This is close to our earlier estimate of the positron lifetime in AlN lattice $\tau_B = 157 \pm 1$ ps.¹³ Typically AlN bulk crystals (measured both here and in earlier samples) show slightly higher $\tau_{ave} = 160$ – 163 ps at RT. The irradiation increased the average lifetime slightly at RT. The average positron lifetime as a function of measurement temperature for a typical as-grown sample and an irradiated sample is shown in Fig. 1. The average lifetime is above the value of the AlN lattice, indicating that vacancies are present in the samples. The increase of average positron lifetime above RT is due to the thermal escape of positrons from shallow states at negative ions, increasing the annihilation signal from the vacancies. In the case of the irradiated sample the increase is more rapid, and at 600 K the average lifetime (190 ps) is higher than in the case of the as-grown sample (181 ps) due to the defects generated by the irradiation. The average lifetime in the as-grown samples is still increasing at 760 K, but the rate of increase is less than at 400–600 K. The positron annihilation spectra can be decomposed into components at temperatures 500–600 K for the as-grown sample and above 300 K for the irradiated sample. The longer lifetime component of the decomposition $\tau_2 = 210 \pm 5$ can be attributed to the AlN vacancy.¹³ The behavior of the average lifetime as a function of measurement temperature is a clear indication that the detected vacancies are in the negative charge state, and that there are negative ions

present in the sample acting as shallow traps for positrons.¹¹ The decomposition of the lifetimes was not possible above 600 K due to the use of a different spectrometer for the high T experiments.

The temperature dependence of the average lifetime can be modeled using the kinetic trapping model for positrons.¹⁸ The average lifetime can be written as $\tau_{ave} = (1 - \eta_V)\tau_B + \eta_V\tau_V$, where τ_B and τ_V are the positron lifetimes in the AlN lattice and the Al vacancy, respectively, and η_V is the annihilation fraction at Al vacancies given by $\eta_V = \kappa_V/(\tau_B^{-1} + \kappa_V)$. The trapping rate κ_V is related to the vacancy concentration through $\kappa_V = \mu_V[V]/N_{at}$, where μ_V is the positron trapping coefficient, $[V]$ is the vacancy concentration, and $N_{at} = 9.6 \times 10^{22} \text{ cm}^{-3}$ is the atomic density of AlN. Vacancy and negative ion concentrations, and also the binding energy of positrons to the negative ions, can be obtained from the behavior of the average lifetime by taking into account also the thermal escape from the Rydberg states of the negative ions.²⁴

The trapping model with negatively charged vacancies and negative ions fits well to the experimental data in Fig. 1. For the as-grown sample we obtained an Al vacancy concentration of $1 \times 10^{18} \text{ cm}^{-3}$ and a negative ion concentration of $1 \times 10^{19} \text{ cm}^{-3}$. Here we have used $\mu_V = 3 \times 10^{15} \times (\frac{300\text{K}}{T})^{1/2} \text{ s}^{-1}$ for the negative defects.²⁵ In the case of the irradiated samples, the fit gives concentrations of $4 \times 10^{18} \text{ cm}^{-3}$ and $3 \times 10^{19} \text{ cm}^{-3}$ for vacancies and negative ions, respectively, with the Al vacancy concentration being in good agreement with the SRIM estimate. The fit deviates from the experimental data slightly above 400 K. This is due to a slight recovery of the irradiation damage starting at above 400 K, and is observable as a decrease of τ_{ave} by 3 ps at RT after the measurement at 600 K. This behavior is, however, the only effect on the data: The τ_{ave} versus T after measuring the irradiated sample at 600 K is qualitatively similar (not shown) to that measured right after irradiation. The positron binding energy to the shallow traps (negative ions) is $E_b = 140 \pm 5$ meV in both cases. The high binding energy suggests that the negative ions are in the 2- charge state.²⁴

Coincidence Doppler measurements were performed in order to obtain direct evidence of the chemical surroundings of the Al vacancy. The measurements were performed at 600 K for the as-grown sample in order to minimize the effect of the the negative ions, and at 400 K for the irradiated sample in order to avoid recovery of the defects. Based on the lifetime experiments, the annihilation fractions of positrons at Al vacancies are 43% for the as-grown sample at 600 K and 27% for the irradiated sample at 400 K. The annihilation fractions are used to extract the vacancy-specific Doppler spectrum ρ_V through $\rho_{meas} = (1 - \eta_V)\rho_B + \eta_V\rho_V$, where ρ_{meas} is the measured spectrum and ρ_B that specific of the AlN lattice.

Figure 2 shows the experimental coincidence Doppler spectra as a ratio to the spectrum of the AlN lattice (obtained in the AlN crystal with the lowest $\tau_{ave} \approx \tau_B$). The figure also shows theoretical calculations for the isolated V_{Al} , V_{Al-O_N} , V_{Al-V_N} and V_{Al-H} . Clearly the experimental curve of the as-grown sample is in the best agreement with V_{Al-O_N} . Especially the shoulder with intensity ≥ 1 around 1.5 a.u.;

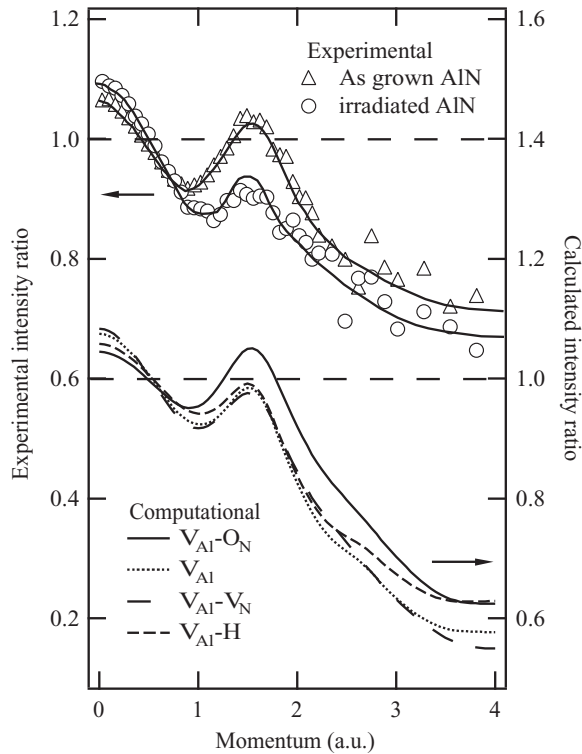


FIG. 2. Experimental (upper panel) and theoretical (lower panel) coincidence intensity ratios for V_{Al} and $V_{\text{Al}}\text{-O}_{\text{N}}$ relative to defect free AlN. The gray lines are drawn to guide the eye.

it is unique to O decoration of the Al vacancy. It should be noted that this is a typical effect of O in III nitrides in general: A similar shoulder of increased intensity is seen in GaN (Ref. 26) and InN (Ref. 27)—the contribution of $2p$ electrons is important in this part of the spectrum. Also, the slightly higher intensity at higher momenta (2–4 a.u.) and lower intensity at zero momentum fits perfectly with $V_{\text{Al}}\text{-O}_{\text{N}}$ in the as-grown sample. Adding more O atoms increases the height of the shoulder even more (not shown for clarity), suggesting that there is only a single O atom neighboring the Al vacancy. In the irradiated sample, the possibility that part of the Al vacancies are decorated by V_{N} (i.e., $V_{\text{Al}}\text{-V}_{\text{N}}$ complexes) cannot be ruled out, but should be unlikely due to the good agreement with the estimated monovacancy production. In any case, the concentration of irradiation-induced Al vacancies is four times higher than that of the in-grown $V_{\text{Al}}\text{-O}_{\text{N}}$, and hence the Doppler spectrum is dominated by the irradiation-induced V_{Al} . In addition, the Doppler spectrum is dominated by $V_{\text{Al}}\text{-O}_{\text{N}}$ in the as-grown material, indicating that this is the dominant form of in-grown V_{Al} .

We performed optical absorption measurements on both as-grown and proton irradiated samples at wavelengths 800–260 nm. The transmission coefficient and the uncorrected (reflectance not taken into account) absorption coefficient are shown in Fig. 3. Notable features of the irradiated sample spectrum include the disappearance of the shoulder at 2.5–3.1 eV and an additional absorption peak at 3.4 eV. The reduction of the shoulder at 2.5–3.1 eV is probably due to a Fermi-level-movement related change in electron occupation of a deep level in the upper part of the band gap. On the other

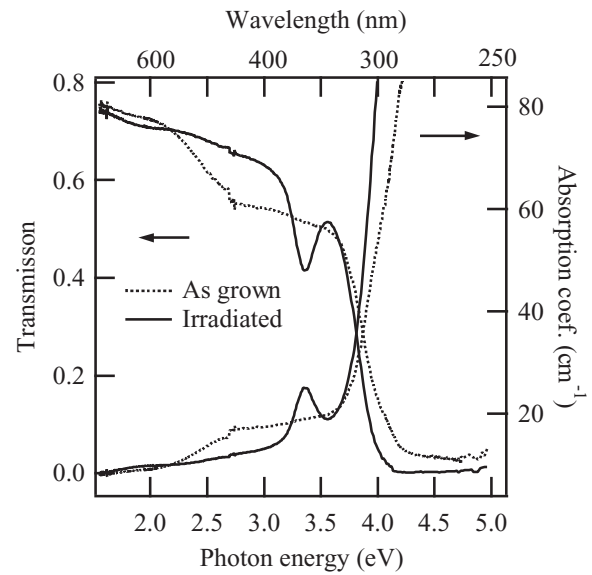


FIG. 3. Transmission coefficient (left axis) and uncorrected absorption coefficient (right axis).

hand, the absorption peak at 3.4 eV (365 nm) is clearly due to a transition between two localized states. Of the defect species generated during the proton irradiation, Al vacancies (V_{Al}^{3-}) have been theoretically predicted to have an energy level at around 2.0–2.5 eV above the valence-band edge (VBE),^{28,29} whereas N vacancies have an energy level at around 5.9 eV above the VBE.³⁰ Hence it is evident that the transition involves V_{Al} and some unidentified donor: V_{N} is a good candidate as they are rather certainly introduced by the irradiation as well. The increase in the absorption observed above 4.0 eV may also be related to V_{Al} , but conclusive evidence cannot be obtained due to the high position-related variation at these wavelengths.

Defect complexes such as $V_{\text{Al}}\text{-O}_{\text{N}}$ and $V_{\text{Al}}\text{-2O}_{\text{N}}$ have been reported to cause absorption in the deep UV,¹⁰ but our results suggest that isolated Al vacancies can also cause absorption at these wavelengths. Interestingly, the comparison of the GDMS-estimated O concentration ($\leq 10^{18} \text{ cm}^{-3}$) and the $V_{\text{Al}}\text{-O}_{\text{N}}$ concentration (10^{18} cm^{-3}) indicates that most, if not all, of the O atoms have a neighboring Al vacancy in as-grown single-crystal AlN. This is very different from, e.g., GaN, where typically $[V_{\text{Ga}}\text{-O}_{\text{N}}] \approx 0.01 \times [\text{O}]$ for O concentrations well above 10^{17} cm^{-3} .

In summary, we have studied in-grown and irradiation-induced Al vacancies in AlN single crystals. By combining coincidence Doppler broadening spectroscopy with *ab initio* calculations, the as-grown samples were found to contain $V_{\text{Al}}\text{-O}_{\text{N}}$ vacancy complexes (concentration $1 \times 10^{18} \text{ cm}^{-3}$) as the dominant form of V_{Al} , whereas irradiation introduces isolated V_{Al} . Our results indicate that UV absorption is caused by Al vacancies, and that most if not all of the O atoms have a neighboring Al vacancy. Hence reducing O concentration in AlN should lead to improved UV transparency.

The authors wish to thank M. Mattila for help with the absorption measurement setup. This work was partially funded by the Academy of Finland and the MIDE programme of Aalto University.

*jussi-matti.maki@aalto.fi

- ¹Y. Taniyasu, M. Kasu, and T. Makimoto, *Nature* **311**, 325 (2006).
- ²H. Morkoç, *Mater. Sci. Eng. R* **33**, 135 (2001).
- ³M. Bickermann, B. M. Epelbaum, and A. Winnacker, *J. Cryst. Growth* **269**, 432 (2004).
- ⁴A. S. Segal, S. Y. Karpov, Y. N. Makarov, E. N. Mokhov, A. D. Roenkov, M. G. Ramm, and Y. A. Vodakov, *J. Cryst. Growth* **211**, 68 (2000).
- ⁵R. Schlessner, R. Dalmau, and Z. Sitar, *J. Cryst. Growth* **241**, 416 (2002).
- ⁶B. M. Epelbaum, C. Seitz, A. Magerl, M. Bickermann, and A. Winnacker, *J. Cryst. Growth* **265**, 577 (2004).
- ⁷J. C. Rojo, G. A. Slack, K. Morgan, B. Raghathamachar, M. Dudley, and L. J. Schowalter, *J. Cryst. Growth* **231**, 317 (2001).
- ⁸M. P. Borom, G. A. Slack, and J. W. Szymaszek, *Am. Ceram. Soc. Bull.* **51**, 852 (1972).
- ⁹G. A. Slack, L. J. Schowalter, D. Morelli, and J. A. Freitas, *J. Cryst. Growth* **246**, 287 (2002).
- ¹⁰P. Lu, R. Collazo, R. F. Dalmau, G. Durkaya, N. Dietz, and Z. Sitar, *Appl. Phys. Lett.* **93**, 131922 (2008).
- ¹¹K. Saarinen, T. Laine, S. Kuisma, J. Nissila, P. Hautojärvi, L. Dobrzynski, J. M. Baranowski, K. Pakula, R. Stepniewski, M. Wojdak, A. Wyszomolek, T. Suski, M. Leszczynski, I. Grzegory, and S. Porowski, *Phys. Rev. Lett.* **79**, 3030 (1997).
- ¹²A. Pelli, K. Saarinen, F. Tuomisto, S. Ruffenach, and O. Briot, *Appl. Phys. Lett.* **89**, 011911 (2006).
- ¹³F. Tuomisto, J.-M. Mäki, T. Yu. Chemekova, Yu.N. Makarov, O. V. Avdeev, E. N. Mokhov, A. S. Segal, M. G. Ramm, S. Davis, G. Huminic, H. Helava, M. Bickermann, and B. M. Epelbaum, *J. Cryst. Growth* **310**, 3998 (2008).
- ¹⁴T. Koyama, M. Sugawara, T. Hoshi, A. Uedono, J. F. Kaeding, R. Sharma, S. Nakamura, and S. F. Chichibu, *Appl. Phys. Lett.* **90**, 241914 (2007).
- ¹⁵J.-M. Mäki, F. Tuomisto, B. Bastek, F. Bertam, J. Christen, A. Dadgar, and A. Krost, *Phys. Status Solidi C* **6**, 2575 (2009).
- ¹⁶A. Uedono, S. Ishibashi, S. Keller, C. Moe, P. Cantu, T. M. Katona, D. S. Kamber, Y. Wu, E. Letts, S. A. Newman, S. Nakamura, J. S. Speck, U. K. Mishra, S. P. DenBaars, T. Onuma, and S. F. Chichibu, *J. Appl. Phys.* **105**, 054501 (2009).
- ¹⁷E. N. Mokhov, O. V. Avdeev, I. S. Barash, T. Yu. Chemekova, A. D. Roenkov, A. S. Segal, A. A. Wolfson, Yu.N. Makarov, M. G. Ramm, and H. Helava, *J. Cryst. Growth* **281**, 93 (2005).
- ¹⁸K. Saarinen, P. Hautojärvi, and C. Corbel, in *Identification of Defects in Semiconductors*, edited by M. Stavola (Academic Press, New York, 1998), p. 209.
- ¹⁹P. E. Blöchl, *Phys. Rev. B* **50**, 17953 (1994).
- ²⁰G. Kresse and J. Furthmüller, *Phys. Rev. B* **54**, 11169 (1996).
- ²¹I. Makkonen, M. Hakala, and M. J. Puska, *Phys. Rev. B* **73**, 035103 (2006).
- ²²S. Väyrynen, P. Pusa, P. Sane, P. Tikkanen, J. Räisänen, K. Kuitunen, F. Tuomisto, J. Härkönen, I. Kassamakov, E. Tuominen, and E. Tuovinen, *Nucl. Instrum. Methods Phys. Res. Sect. A* **572**, 978 (2007).
- ²³J. P. Biersack and W. Eckstein, *Appl. Phys. A* **34**, 73 (1984).
- ²⁴F. Tuomisto, V. Ranki, D. C. Look, and G. C. Farlow, *Phys. Rev. B* **76**, 165207 (2007).
- ²⁵P. Hautojärvi and C. Corbel, *Positron spectroscopy at defects in metals and semiconductors*, Proc. Int. School of Physics Enrico Fermi Course CXXV (IOS Press, Amsterdam, 1995), pp. 491–532.
- ²⁶S. Hautakangas, I. Makkonen, V. Ranki, M. J. Puska, K. Saarinen, X. Xu, and D. C. Look, *Phys. Rev. B* **73**, 193301 (2006).
- ²⁷C. Rauch, I. Makkonen, and F. Tuomisto, *Phys. Rev. B*, e-print [arXiv:1104.2498](https://arxiv.org/abs/1104.2498) (2011).
- ²⁸C. Stampfl and C. G. Van de Walle, *Phys. Rev. B* **65**, 155212 (2002).
- ²⁹Y. Zhang, W. Liu, and H. Niu, *Phys. Rev. B* **77**, 035201 (2008).
- ³⁰N. Nepal, K. B. Nam, M. L. Nakarmi, J. Y. Lin, H. X. Jiang, J. M. Zavada, and R. G. Wilson, *Appl. Phys. Lett.* **84**, 1090 (2004).